

RESEARCH

Open Access



Curcumin-polyvinyl alcohol nano-composite enhances tolerance of *Helianthus annuus* L. against salinity stress

Faten S. Zaki¹, Mahmoud A. Khater^{1*} , Mohamed E. El-Awadi¹, Mona G. Dawood¹ and Alaa E. Elsayed²

Abstract

Background Nanotechnology is a promising technology in many fields including agriculture. So, this investigation aimed to study effect of curcumin (CUR) with polyvinyl alcohol (PVA) nano-composite at 0, 20, 40 and 60 mg L⁻¹ on physiochemical attributes of sunflower plants grown under salinity stress (3000 ppm).

Results Results showed that salinity stress significantly reduced all growth indices like plant height, number of leaves/plant, fresh and dry weight of shoot and leaf area accompanied by significant increases in proline content, secondary metabolites (total phenolic compound contents and flavonoids), malondialdehyde (MDA) and hydrogen peroxide (H₂O₂). In addition, catalase, peroxidase, superoxide dismutase, and glutathione reductase increased significantly. The decreases in chlorophyll a, chlorophyll b and carotenoids due to salinity stress were non-significant. On the other hand, curcumin with polyvinyl alcohol (CUR-PVA) nano-composite at all concentrations significantly promoted all vegetative growth parameters, total photosynthetic pigments, secondary metabolites, antioxidant enzyme activities accompanied by significant decreases in proline content, MDA and H₂O₂ either in plant irrigated with tap water or saline solution relative to corresponding control. CUR-PVA nano-composite at 20 mg L⁻¹ was the most optimum treatment either in plant irrigated with tap water or saline solution since it caused the highest significant increases in vegetative growth parameters, total photosynthetic pigments, secondary metabolites and antioxidant enzyme activities accompanied by highest significant decreases in proline content, MDA and H₂O₂ relative to control.

Conclusions In brief that CUR-PVA nano-composite employs no noticeable effect in decreasing the deleterious effect of salinity on quality of sunflower.

Keywords Sunflower, Salt stress, Curcumin, Polyphenol, Nanoparticles, Antioxidant

1 Background

The most important oil-producing crop that can be grown in different types of soils and climates is sunflower (*Helianthus annuus* L.). Sunflower is one of the most promising renewable energy options due to its high

biomass and biofuel. Sunflower can be grown two times a year due to its brief developing season (ninety-one hundred twenty days). Seeds of sunflower comprise high oil (25–48%) and protein (20–27%) percentage. Owing to its excessive content of mono- and polyunsaturated fatty acids and low content of saturated fatty acids, sunflower oil is a high-quality vegetable oil [1, 2]. It is important to note that sunflower plant is considered to be a crop with a moderate tolerance to salt.

Salt stress is a major abiotic stress resulting from constant climate change and environmental deterioration caused by human activities across the globe. Salinity had a negative impact on a selection of metabolic activities

*Correspondence:

Mahmoud A. Khater
mahmoudkhater2000@gmail.com

¹ Botany Department, Agriculture and Biological Institute, National Research Centre, Giza, Egypt

² Polymers and Pigments Department, National Research Centre, Giza, Egypt

such as photosynthesis, respiration, transpiration, nutrient balance, membrane properties, enzymatic activities, cellular homeostasis and hormone balance. These results then had an impact on seed germination, plant growth and productivity as well as reduced the quality of crop products [3, 4]. The osmotic, ionic and nutritional homeostasis of plants may be modified in step with overabundance of Na^+ and Cl^- ions in the root region [5]. Reactive oxygen species (ROS) were produced as a result of salt stress, and these ROS seriously damaged the membrane lipids, proteins, nucleic acids, and photosynthetic machinery [3].

Plants have developed a number of defense mechanisms to survive in saline environments in order to escape the damaging consequences of salinity, such as the accumulation of osmolytes (proline) and secondary metabolites (phenolic compounds) [6]. According to Mansour and Ali [7], proline maintains cell turgidity, cellular homeostasis and protected protein function during stress recovery process [8]. Phenolic compounds can be concerned within hydrogen peroxide scavenging cascade in plant cells with regard to secondary metabolites [9]. Additionally, flavonoids (secondary metabolic compounds) play a crucial physiological function in the ability of plants to withstand stress by scavenging oxidizing molecules like singlet oxygen and free radicals [10]. Antioxidant enzymes superoxide dismutase (SOD), catalase (CAT) and ascorbate peroxidase (APX) performs a critical role in ROS scavenging. Lipid peroxidation may be avoided by way of the movement of SOD which converts superoxide anions into hydrogen peroxide (H_2O_2) then H_2O_2 is transformed to H_2O with the aid of CAT and APX [11].

Turmeric (*Curcuma longa* L.) is an extensive spread spice determined in conventional Indian and Chinese drug treatments. Curcumin (CUR) is a polyphenol curcuminoid of turmeric rhizome, a member of the ginger family (*Zingiberaceae*). Chemical name of CUR is 1, 7-Bis (4-Hydroxy-3-Methoxyphenyl)-1, 6-Heptadiene-3, 5-Dione. CUR (diferuloylmethane) is a low molecular weight brightly yellow pigment. Two ferulic acids in CUR bound with two carboxyl groups via methylene bridges [12, 13]. Aromatic ring structure in CUR contains o-methoxy phenolic corporations connected by a seven carbon spacer consisting of α , β -unsaturated β -diketone moiety [14]. Among the keto and the enol tautomer, CUR exists in stability. Cur's enol shape is almost the best shape of the molecule in solution [15]. Like other polyphenols, CUR is a strong antioxidant [16]. Since CUR has two phenolic sites and can thus immediately scavenge free radicals. The production of reactive oxygen species (ROS) and reactive nitrogen species (RNS) within the cellular surroundings has been efficaciously inhibited by

means of CUR. Superoxide dismutase and glutathione peroxidase, two first line enzymes of defense against oxygen free radicals, are regulated by the CUR. CUR exhibits anti-inflammatory, anticancer, antioxidant, antiviral, antimicrobial and anti-parasitic activities [17]. In vivo and in vitro studies revealed that the therapeutic potential of CUR has no negative effects on animal models [18].

Due to its poor aqueous solubility, CUR fails to exert its biological activity [19]. To overcome this problem, nanotechnology is used to enhance its physicochemical properties regarding its efficacy [20]. Nanotechnology is a promising technology in many fields including agriculture [21]. The main possible way for application of nanoparticles on plants is through foliar application. Since the primary functions of plant's leaves are photosynthesis, transpiration, and gas exchange [22]. Solvent evaporation, nano-precipitation, emulsification, salting-out and dialysis are some techniques used in nano preparation [23]. Ke et al. [24] succeeded to increase CUR-loaded nanoparticles with the aid of dissolving CUR in water, cyclopentanone and surfactants. Many studies showed that nanoparticles of curcumin have active treatment for several sicknesses.

Quite a lot of research paper deals with the effect of curcumin on animal system whereas; a few searches have been done on the role of curcumin on plant. Consequently, the principle aim of this search is to create a singular nano formulation for CUR transport thru PVA-primarily based hydrogen bonding interactions. The ensuing CUR-PVA nano-composite used as an try in amelioration of salinity stress on a few physiological and biochemical adjustments of sunflower vegetation.

2 Methods

CUR (purity $\geq 65\%$), polyvinyl alcohol (PVA, 87–89% hydrolyzed) and polysorbates (tween 20 and 80) were from Sigma Aldrich (St Louis, MO, USA.). NaOH and sodium dodecyl sulfate (SDS) were purchased from El-Nasr Company for Pharmaceutical Industries.

2.1 CUR-PVA nano-composite preparation

CUR nano-composite was prepared from ethanol extract of crude powder of Cur by mixing 200 g of CUR in 800 ml of 98% ethanol via high speed mixture [25]. Liquid phase was evaporated at room temperature in petri dishes. The resultant powder was preserved in a sterile glass bottle at room temperature till used for preparing the nano-composite. Oil water nano-composite was prepared by mixing oil phase of ethanol extract in aqueous phase containing 3%(v/v) Tween 20, 3%(v/v) Tween 80 (based on the oil phase) and SDS (5%) dissolved in phosphate buffer solution at pH 7 and stirred using high speed homogenizer (3000 rpm) for at 30 min to ensure

complete hydration. After complete emulsification, speed was slowed down 1000 rpm and PVA solution (0.6 mg/ml, pH 7) was added gradually for 15 min. The free Cur was then removed by ultracentrifugation at 2500 rpm for 30 min. The final product was a stable emulsion containing 20% ethanol extract of Cur covered with PVA.

2.2 Characterization techniques

2.2.1 Fourier-transform infrared (FT-IR) spectroscopy

ATR-FTIR was measured by Bruker VERTEX 80 (Germany) joint Platinum Diamond ATR comprises a diamond disk as that of an internal reflector in the range 400–4000 cm^{-1} with resolution 4 cm^{-1} , refractive index 2.4.

2.2.2 X-ray diffraction (XRD)

XRD was done using a pan analytical XRD model X Pert PRO with secondary monochromator, CU-radiation = 1.542 Å at 35 mA and 45 kV and scanning speed 0.04°/sec were used.

2.2.3 Measurement of particle size, zeta potential and Transmission electron microscope (TEM) imaging

CUR-PVA nano-composite was characterized using TEM and dynamic light scattering (DLS) by using Zeta Sizer Nano-ZS90 (Malvern Instruments, Ltd., UK) to assess the particle size, size distribution and zeta potential (surface charge) of the prepared nanoparticles.

2.2.4 Plant material and growth conditions

To assess the influence of foliar applied varying levels of CUR-PVA nano-composite (0, 20, 40, 60 mg L^{-1}) on different physiological and biochemical attributes of sunflower (*Helianthus annuus* L.) under salinity (3000 mg L^{-1}). Two pot experiments were conducted at the greenhouse of Botany Department, National Research Centre, Dokki, Cairo, Egypt at the summer seasons of 2020 and 2021. Seeds of sunflower (*Helianthus annuus* L., cultivar Sakha 53) were supplied by Agricultural Research Centre, Giza, Egypt. A factorial experiment with two factors (salinity as main factor and CUR-PVA nano-composite as sub main factor) were arranged in a complete randomized block design with six replicates per treatment. Seeds were planted in pots (35 cm^3). The physical and chemical properties of studied soil were determined and presented in Table 1. After three weeks of growth, the pots (each pot contain 3 plants) were divided into two main groups according to irrigation with saline solutions by using full strength Hoagland's nutrient solution at 0 and 3000 mg L^{-1} . Each group was divided into four sub-groups of different concentrations of CUR-PVA nano-composite (0, 20, 40 and 60 mg L^{-1}). After 21 days from sowing, the seedlings were thinned to three seedlings per

Table 1 Physiological and chemical analysis of soil

Characteristics	Value
Physical properties	
Particle size distribution	
Coarse Sand%	73.8
Fine Sand%	15.5
Silt%	6.5
Clay%	4.2
Texture Soil	Sandy
Chemical properties	
Organic matter content%	1.24
pH	7.8
EC ds/m	0.74
Cations meq/L	
Na ⁺	4.15
K ⁺	0.23
Ca ⁺⁺	1.84
Mg ⁺⁺	1.25
Anions meq/L	
HCO ₃	0.64
CO ₃	Nil
SO ₄	0.93
Cl ⁻	5.6

pot and plants were irrigated with saline solution. Each pot received the same volume of saline solutions for three times, whereas tap water was used for the fourth one to prevent accumulation of salts around root system. Fertilization was done according to recommendation of Agricultural ministry.

2.2.5 Vegetative growth parameters

Plant samples were gathered from each treatment after 50 days from sowing to determine physiological and biochemical analysis. The growth parameters were plant height (cm), number of leaves/plant, shoot fresh weight (FW) (g), shoot dry weight (DW) (g) and leaf area (LA) (cm^2/plant). Dry weight was measured by drying plant sample in oven for 48 h at 50 °C and then weighted.

2.3 Biochemical analysis

2.3.1 Photosynthetic pigment

For chlorophyll a, b and carotenoid contents, the method proposed by Moran and Porath [26] was used. Fresh fully mature leaf (50 mg) samples from each treatment were mixed with 10 ml N–N dimethyl formamide and placed in a refrigerator for 24 h. Following the centrifugation at 4000 × g for 15 min, the optical density was calculated using JASCO V-750 spectrophotometer.

2.3.2 Proline content

The proline content was determined by acid-ninhydrin procedure of Bates et al. [27] on the youngest fully expanded leaves. 0.5 g of fresh leaves from each treatment were homogenized in 3% (w/v) sulphosalicylic acid, and then centrifuged at 3000 rpm for 5 min. 2.0 ml supernatant was mixed to 2.0 ml of ninhydrin reagent and 2.0 ml of glacial acetic acid and incubated at 100 °C for 1 h before being cooled in an ice bath for 15 min. As a reaction reagent, 4.0 ml toluene was added to the previous mixture, and the absorbance was measured at 520 nm using JASCO V-750 spectrophotometer. The proline content was determined using the standard curve and expressed as nmol/g FW.

2.3.3 Total phenolic compounds (TPC) and total flavonoid contents (TFC)

The dried leaf samples were ground into a powder using a small crusher. For each treatment 1 g of powdered leaves was extracted with 100 ml methanol (80%). The mixtures were centrifuged for 3 min at 4 °C at 4000 × g.

TPC was determined using a Folin–Ciocalteu colorimetric assay modified by Elzaawely and Tawata [28]. To 0.2 ml extract, 0.5 ml of distilled water and 0.5 ml Folin–Ciocalteu reagent was added. After 5 min, 1 ml of 7% Na₂CO₃ was added to the mixture. After incubation at room temperature for 90 min, the absorbance was measured at 765 nm with a JASCO V-750 spectrophotometer. TPC was calculated from a standard curve of gallic acid and expressed as mg gallic acid equivalent /g DW.

TFC of each extract was determined using the aluminum chloride technique modified by Chang et al. [29]. 2 ml extract was mixed with 1.5 ml of methanol and 0.1 ml of 10% aluminum chloride and 0.1 ml 1 M potassium acetate and 2.8 ml distilled water. It was left at room temperature for 30 min then absorbance was measured at 415 nm against the blank. TFC was calculated from a standard curve of quercetin and expressed as mg quercetin equivalent/g DW.

2.3.4 Lipid peroxidation and hydrogen peroxide contents

Lipid peroxidation level was measured by determining the level of malondialdehyde (MDA) content using the method of Heath and Packer [30]. 0.5 g fresh leaf sample was homogenized in 10 ml of 5% tri-chloroacetic acid (TCA). The homogenate was centrifuged at 15,000 × g for 10 min. 4.0 ml of 0.5% thiobarbituric acid (TBA) in 20% TCA was added to 2.0 ml of the supernatant. The mixture was heated at 95 °C for 30 min and then quickly cooled in an ice bath and centrifuged at 10,000 × g for 10 min. The absorbance was recorded at 500 nm and for non-specific absorption at 600 nm by JASCO V-750

spectrophotometer. The MDA concentration was calculated using an extinction coefficient 155 mmol L⁻¹ cm⁻¹ and expressed as nmol (MDA) g⁻¹ FW.

Hydrogen peroxide (H₂O₂) in the samples was determined following the method of Yu et al. [31]. 0.5 g fresh leaf tissue was ground in a pre-chilled mortar with 5.0 ml of 0.1% (w/v) TCA. After centrifugation at 12,000 × g for 15 min, 0.5 ml of supernatant was added to 0.5 ml of potassium phosphate buffer (pH 7.0) and 1.0 ml of potassium iodide (KI). The absorbance was measured at 390 nm by JASCO V-750 spectrophotometer. The amount of H₂O₂ was calculated using the extinction coefficient 0.28 μm⁻¹ cm⁻¹ and expressed as nmol g⁻¹ FW.

2.3.5 Antioxidant enzyme activities

The fresh sunflower leaves (1 g FW) from each treatment were placed into liquid nitrogen and then homogenized in ice cold phosphate buffer (50 mM, pH 7.8), with the addition of 1 mM EDTA and 1% (w/v) insoluble polyvinyl polypyrrolidone (PVPP) followed by centrifugation at 15,000 rpm at 4 °C for 20 min. The supernatant was used for the assay of enzyme activities. The activities of CAT, POX, SOD and GR were performed spectrophotometrically with JASCO V-750.

Catalase (CAT, EC 1.11.1.6) activity was determined by following the decrease in absorbance at 240 nm. The mixture (3 ml) contained 1.9 ml phosphate buffer (50 mM, pH 7), 100 μl enzyme extract and 1 ml 0.3% H₂O₂. The reaction was initiated by adding enzyme extract [32].

Peroxidase (POX, EC 1.11.1.7) activity was measured using the method of Kumar and Khan [33]. The reaction mixture contained 2 ml of 0.1 M phosphate buffer (pH 6.8), 1 ml of 0.01 pyrogallol, 1 ml of 0.005 M H₂O₂ and 0.5 ml of enzyme extract. The mixture incubated for 5 min at 25 °C after which 1 ml of 2.5 N H₂SO₄ was added. POX was determined by measuring absorbance at 420 nm against blank.

Superoxide dismutase (SOD, EC 1.12.1.1) was assayed at 560 nm by nitro-blue-tetrazolium (NBT) reduction according to the method of Chen and Wang [32]. The reaction mixture (3 ml) contained 150 μ riboflavin (13 μM), 2.5 ml methionine (13 μM), 250 μ NBT (63 μM), 50 μ phosphate buffer (50 mM, pH 7.8) and 50 μ enzyme extract. One unit of SOD activity was defined as the amount of enzyme required for inhibition of 50% reduction of NBT.

Glutathione reductase (GR, EC 1.8.1.7) was estimated according to Rao et al. [34] by following the increase in absorbance at 340 nm. 2 ml reaction mixture contained 50 mM Tris–HCl (pH 7.5), 0.15 mM NADPH₂, 0.5 mM oxidized glutathione (GSSG) and 3 mM MgCl₂. The oxidation of NADPH₂ was recorded for 3 min after adding 200 μl of enzyme extract.

2.3.6 Extraction of proteins and SDS-PAGE analysis

Proteins were extracted from fresh leaves and the extraction technique was similar to the extraction technique described by Saraswati et al. [35]. Protein profiling of samples was performed using SDS-PAGE as described by Laemmli [36].

2.3.7 DNA isolation and PCR

Total genomic DNA was isolated from young leaves of treated sunflower plants according to modified CTAB method described by Khaled and Esh [37]. Five ISSR primers, as shown in Table 2 were used in this study to determine the molecular differences or variations between treated sunflower plants. Moreover, polymerase chain reaction (PCR) was carried out within 15 µl reaction volumes, containing 1 µl plant genomic DNA, 7.5 µL Master Mix (Gene Direx one PCRTM), 1 µL template DNA and 1 µL primer.

PCR was programmed as: an initial denaturation at 94 °C for 5 min, 35 cycles each of 94 °C for 1 min, 55 °C

for 1 min, 72 °C for 2 min and final extension at 72 °C for 10 min. Amplification products were electrophoresed on 1.5% agarose in 1×TAE buffer. Then gel was stained with ethidium bromide and documented using gel documentation system.

2.4 Statistical analysis

Data average of two seasons was statistically analyzed by analysis of variance. The differences among means were determined by least significant differences (LSD) according to Silva and Azevedo [38] with calculated standard deviation (± SD).

3 Results

3.1 Characterization of CUR-PVAnano-composite

3.1.1 FT-IR spectroscopy

FT-IR was applied to estimate the synthesized polymer composites. For curcumin in Fig. 1, the bands at 1436 cm⁻¹ and 1508 cm⁻¹ are associated to olefinic bending vibration of C–H bound to the benzene ring of curcumin and C–C vibrations, respectively [39, 40]. The wide absorption band at 3282 cm⁻¹ is attributed to the phenolic O–H stretching. The bands at 1620 cm⁻¹ and 1613 cm⁻¹ are allied to carbonyl group and stretching vibrations of the benzene ring, respectively. The bands at 1224 cm⁻¹ and 1148 cm⁻¹ are due to aromatic C=O stretching and C–O–C stretching types, respectively [41].

FT-IR of PVA (Fig. 2) band at 3285 cm⁻¹ matching to OH stretching. The Peak at 2909 cm⁻¹ is associated to

Table 2 ISSR primers and their sequences

1	Primer Code	Primer Sequence (5' → 3')	
		(CT)8TG	CTCTCTCTCTCTCTTG
2	HB 8	(GA)6GG	GAG AGA GAG AGA GG
3	HB 10	(GA)6CC	GAG AGA GAG AGA CC
4	HB 12	(CAC)3GC	CAC CAC CACGC
5	HB 15	(GTG)3GC	GTG GTG GTGGC

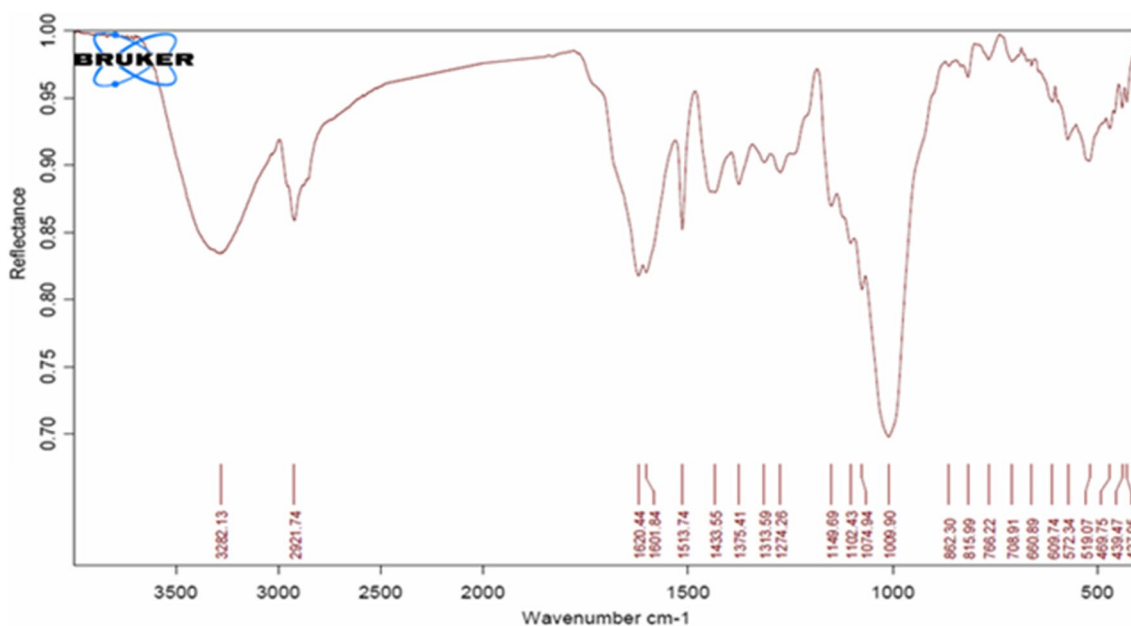


Fig. 1 FT-IR spectra for curcumin (CUR)

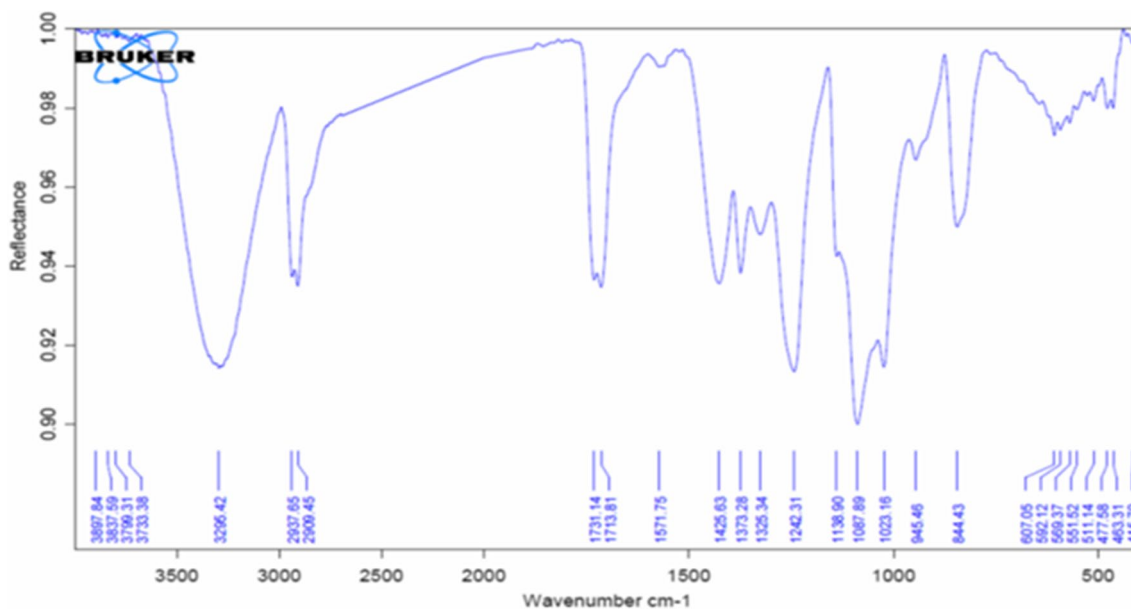


Fig.2 FT-IR spectra for PVA

symmetric/asymmetric C–H stretching. The peak at 1713 cm⁻¹ is attributed to the distortion band of water H–O–H. The peak at 1138 cm⁻¹ is related with C-H overtone vibrations.

FT-IR of curcumin-PVA (Fig. 3) the peak at 3282.4 cm⁻¹ is due to the increased intermolecular H bonding in presence complex. The Shift of peaks in the range of 1000–4000 cm⁻¹ supports the formation of the complex. The peak at 1224 cm⁻¹ and 1508 cm⁻¹ of

curcumin moved to 1373 cm⁻¹ and 1565 cm⁻¹ in the complex, respectively and their intensity decreased which clarifies the formation of the complex. The appearance of the peak at 1565 cm⁻¹ in the complex is allied to the peak at 1613 cm⁻¹ of curcumin. The band at 1585 cm⁻¹ may be related to asymmetrical stretching of carboxylate groups or intramolecularly bound water. The peak at 1400 cm⁻¹ corresponds to symmetrical stretching of carboxylate groups of PVA and the stretching vibration

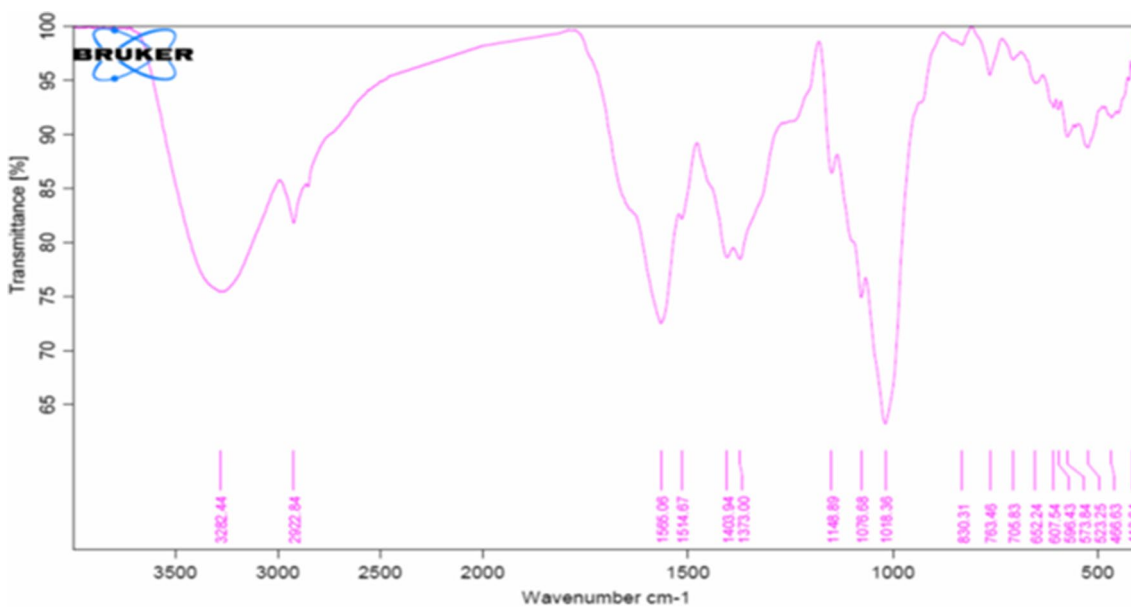


Fig.3 FT-IR spectra for CUR-PVA

of alcoholic groups, respectively. The FT-IR of curcumin PVA nano-composite shows that the peaks at 1373 cm^{-1} and 1514 cm^{-1} were related to curcumin.

From FigS. 1, 2 and 3 peak observed at the range of $800\text{--}1100\text{ cm}^{-1}$ which was correspondent to the stretching mode of vinyl bonds. The -CH stretching vibration of the polymer backbone is established through peaks at 2921 cm^{-1} . The peak at 1601 and 3282 cm^{-1} equivalent to C=O and O-H bending vibrations respectively [42]. The ether bands of the PVA can be obtained near 1100 cm^{-1} spectral region. The broad band showed in the range from 3200 to 3690 cm^{-1} is correlated to the stretching O-H [43].

3.2 XRD analysis

XRD of CUR-PVA are shown in Table 3 and Fig. 4. XRD pattern has amorphous structure and suggests a sharp diffraction peak centered at $2\theta \approx 19^\circ$. CUR is combined into PVA matrix and a true presence complex between CUR and PVA is formed. The hydrophobic compounds such as CUR can make a non-covalent bond with the hydrophilic PVA and form an inclusion complex. In the inclusion complex, the guest molecules are different from

Table 3 XRD peak number, theta, D-spacing of CUR-PVA composite

Peak Number	Pos. [$^{\circ}2\theta$.]	D-spacing	Height [cps]	Rel. Int. [%]
1	19.4999	4.55237	207.41	100.00
2	20.1637	4.40398	160.60	77.43
3	22.8313	3.89510	13.23	6.38
4	40.7765	2.21292	10.18	4.91

each other and therefore cannot form crystals [44]. The XRD configurations of CUR and PVA show amorphous and semi-crystalline structures, respectively.

CUR-PVA nano-composite was successfully prepared via using nano-composite technique using PVA as outer shell agent. CUR-PVA nano-composite was characterized using TEM and DLS by Zeta Sizer Instrument. The TEM image (Fig. 5) showed obviously that CUR-PVA nano particles have spherical shape with an average size $21\text{--}63\text{ nm}$. Effects of DLS (Fig. 6) showed that CUR-PVA nano-composite have slim length distribution with average length of $70\text{--}80\text{ nm}$. The difference in the size of the prepared nano-composite between TEM and DLS may be due to the swelling of CUR-PVA nano-composite in aqueous solution and DLS may be responsible for a hydrodynamic radius of nano-composite, whereas the TEM provides the dried diameter of prepared CUR-PVA nano-composite. In addition, TEM gives an image for selected area for measurements; while, DLS gives an overall image of the nano-composites and their accumulations. Zeta potential of CUR-PVA nano-composite was -34 mv . The negatively charged CUR-PVA nano-composite was due to the anionic nature of surfactant in neutral media. Polydispersity index (PDI) reveal the regularity of particles size and agglomeration, also it give a perfect picture about the particles firmness. PDI from Dynamic Light Scattering DLS is 0.1 which is classified as moderately polydisperse distribution type.

3.3 Vegetative growth parameters

Table 4 indicates that salt stress decreases considerably all morphological parameters i.e. plant height, number of leaves /plant, fresh and dry weight of shoot and leaf

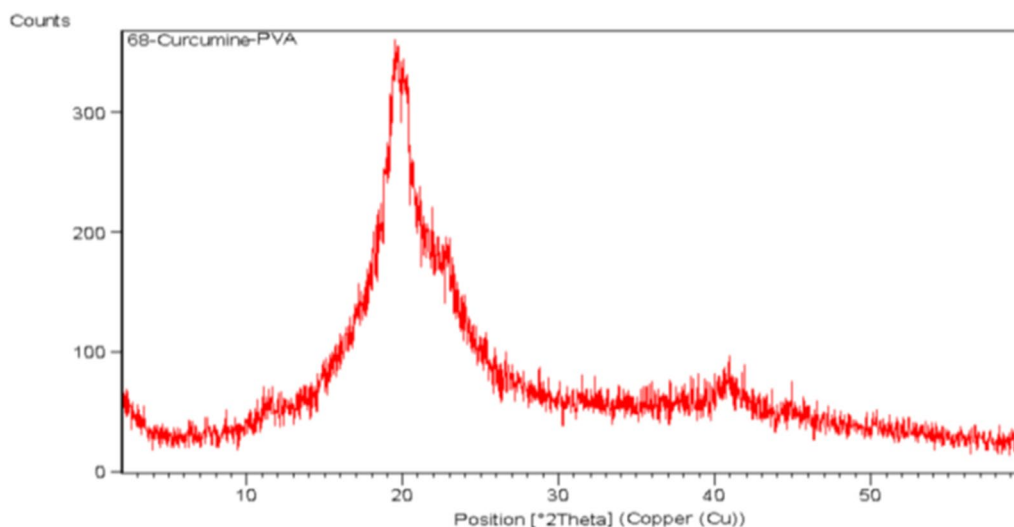


Fig.4 XRD patterns of CUR-PVA composite

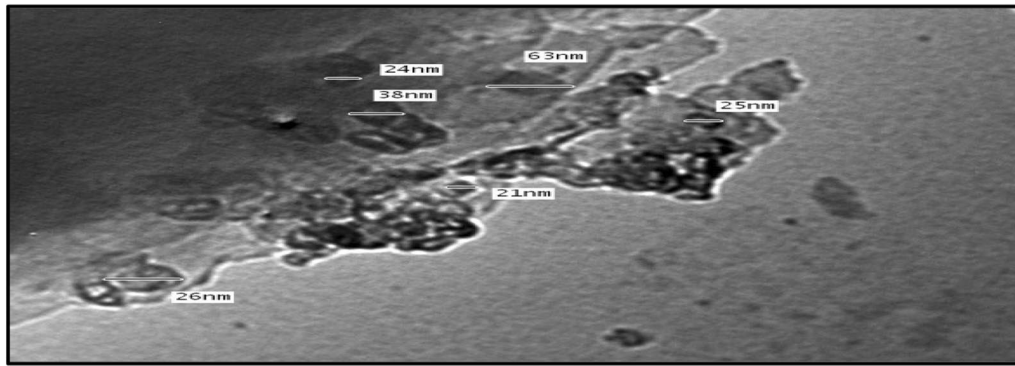


Fig.5 TEM of CUR-PVA nano-composite at scale 100 nm

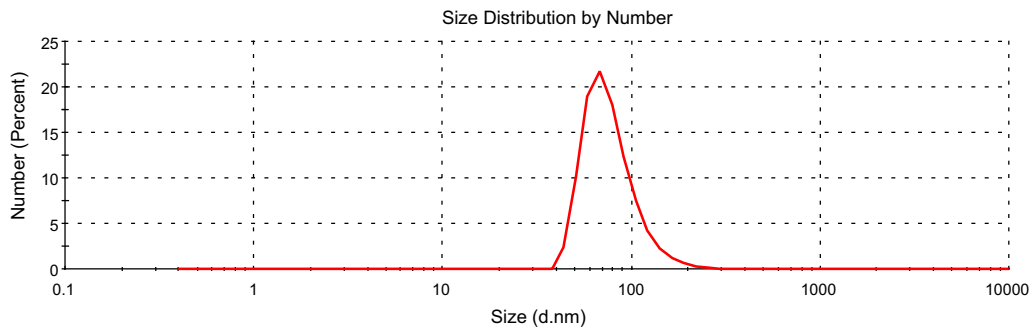


Fig.6 DLS of CUR-PVA nano-composite

Table 4 Effect of CUR-PVA nano-composite (CUR-PVA) concentrations (0, 20, 40 and 60 mg L⁻¹) on growth indices of sunflower cultivated under salt stress (S0, tap water; S1, 3000 ppm)

Treatments	Plant height (cm)	Leaves number/plant	Shoot fresh weight (g)	Shoot dry weight (g)	Leaf area (cm ² /plant)	
S0	43.50	13.66	8.32	4.53	33.65	
S1	37.46	12.16	7.21	3.75	27.00	
LSD 5% level	1.182	1.089	0.945	0.637	2.338	
CUR-PVA (mg L ⁻¹)						
0	33.17	11.67	5.52	2.83	11.67	
20	45.50	13.83	9.86	5.41	13.83	
40	44.00	13.50	8.41	4.52	13.50	
60	39.58	12.67	7.28	3.81	12.67	
LSD 5% level	1.671	1.540	1.337	0.901	3.307	
S0	0	38.67 ± 1.15	12.33 ± 0.58	6.27 ± 1.26	3.37 ± 0.40	12.33 ± 0.58
	20	48.00 ± 1.00	15.00 ± 1.00	10.30 ± 1.17	5.93 ± 1.26	15.00 ± 1.00
	40	47.33 ± 0.58	14.33 ± 0.58	8.44 ± 0.68	4.61 ± 1.19	14.33 ± 0.58
	60	40.00 ± 0.00	13.00 ± 2.05	8.28 ± 1.54	4.20 ± 0.65	13.00 ± 2.05
S1	0	27.67 ± 1.53	11.00 ± 1.00	4.77 ± 1.20	2.29 ± 0.08	11.00 ± 1.00
	20	43.00 ± 3.00	12.67 ± 1.15	9.41 ± 0.31	4.88 ± 0.18	12.67 ± 1.15
	40	40.67 ± 0.58	12.67 ± 1.15	8.38 ± 1.12	4.43 ± 0.62	12.67 ± 1.15
	60	39.17 ± 0.76	12.33 ± 0.58	6.28 ± 0.98	3.42 ± 0.59	12.33 ± 0.58
LSD 5% level	2.364	2.178	1.890	1.275	4.677	

area under investigation. Meanwhile, CUR-PVA nano-composite at all concentrations significantly increased all examined growth parameters. These increases are in opposite direction with CUR-PVA nano-composite concentration. The highest significant increase in these parameters was due to 20 mg L⁻¹ CUR-PVA nano-composite.

Regarding interaction between salinity stress and different concentrations of CUR-PVA nano-composite, it was noted that CUR-PVA nano-composite at 20 and 40 mg L⁻¹ expressively increased all growth indices in plants irrigated with tap water or saline solution comparative to control. Besides, the increase due to CUR-PVA nano-composite at 60 mg L⁻¹ was significant in most parameters. CUR-PVA nano-composite at 20 mg L⁻¹ increased shoot dry weight of plant irrigated with tap water by 75.96% and in plant irrigated with saline solution by 113.10% comparative to control. CUR-PVA nano-composite at 60 mg L⁻¹ increased shoot dry weight of plant irrigated with tap water by 24.63% and in plant irrigated with saline solution by 49.34% comparative to control. Hence, it is obvious that the response of plant irrigated with saline solution to CUR-PVA nano-composite was more pronounce than the response of plant irrigated with tap water.

Figure 7 shows that salinity stress caused non-significant decreases in all photosynthetic components (chlorophyll a, chlorophyll b & carotenoids) relative to control. Meanwhile, CUR-PVA nano-composite at all concentrations considerably increased all photosynthetic components i.e. chlorophyll a, chlorophyll b& carotenoids relative to control. These increases are in opposite direction with CUR-PVA nano-composite concentration i.e., the highest significant increases in these parameters was due 20 mg L⁻¹ CUR-PVA nano-composite.

Regarding interaction between salinity stress and different concentrations of CUR-PVA nano-composite, it was noted that CUR-PVA nano-composite at all concentration significantly increased total photosynthetic pigments in plant irrigated either with tap water or saline solution comparative to control. CUR-PVA nano-composite at 20 mg L⁻¹ increased chlorophyll a, chlorophyll b & carotenoids in plants watered with tap water by 71.44% and in plants watered with saline solution by 100.63% relative to corresponding control.

Figure 8 shows that salinity stress caused significant increases in proline, total phenolic content, flavonoid, malondialdehyde and hydrogen peroxide relative to control. Meanwhile, CUR-PVA nano-composite at all concentrations significantly increased total phenolic content and flavonoid, accompanied by significant decreases in

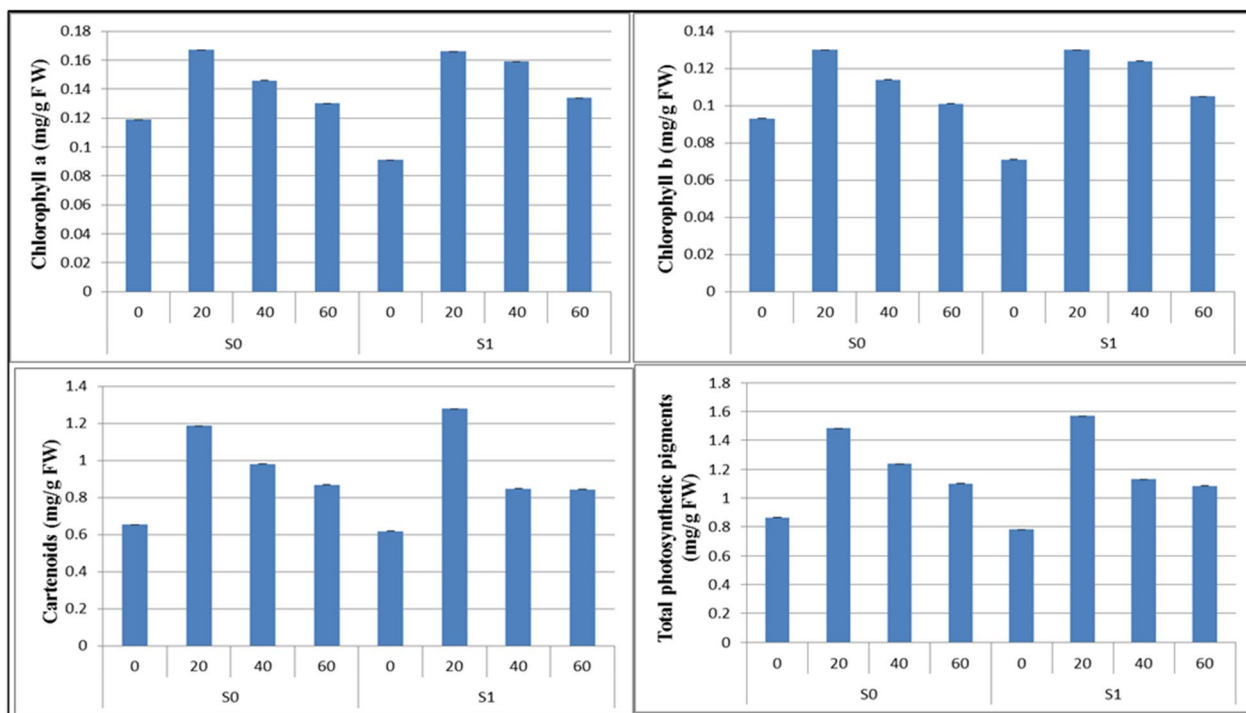


Fig.7 Effect of CUR-PVA nano-composite concentrations (0, 20, 40 and 60 mg L⁻¹) on photosynthetic pigments (mg/g fresh leaf tissue) of sunflower cultivated under salt stress (S0, tap water; S1, 3000 ppm)

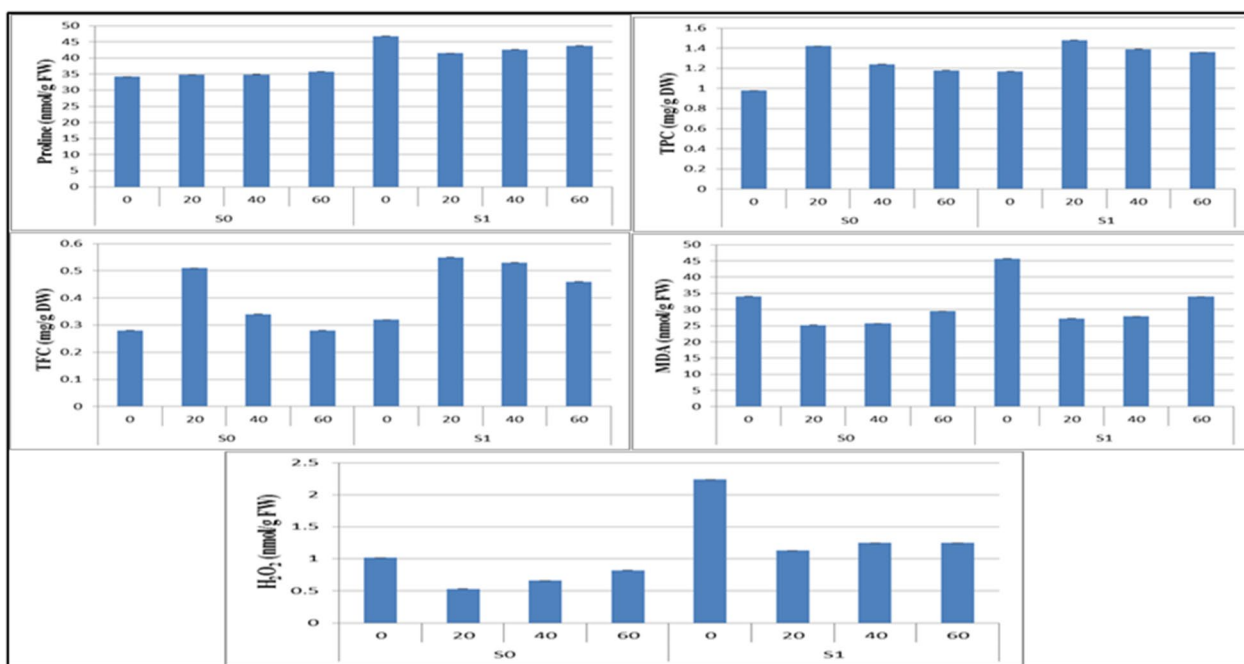


Fig.8 Effect of CUR-PVA nano-composite concentrations (0, 20, 40 and 60 mg L⁻¹) on proline, phenolic content (TPC), flavonoid (TFC), malondialdehyde (MDA), and hydrogen peroxide (H₂O₂) of sunflower cultivated under salt stress (S0, tap water; S1, 3000 ppm)

proline content, malondialdehyde and hydrogen peroxide relative to control. CUR-PVA nano-composite at 20 mg L⁻¹ showed the highest significant increases in total phenolic content and flavonoid, and highest significant decreases in proline content, malondialdehyde and hydrogen peroxide relative to control.

Regarding interaction between salinity stress and different concentrations of CUR-PVA nano-composite, it was noted that CUR-PVA nano-composite at all concentrations caused non-significant increase in proline content in plant watered with tap water and major decreases in plants irrigated with salty solution relation to control. Whereas, total phenolic content and flavonoid were considerably increased due to all applied treatments either in plant irrigated with tap water or saline solution. Malondialdehyde and hydrogen peroxide were significantly decreased due to all applied treatments either in plant watered with tap water or saltwater. The most optimum treatment of CUR-PVA nano-compositewas at 20 mg L⁻¹, whichsignificantly increases the total phenolic content and flavonoid accompanied by the highest significant decrease in malondialdehyde and hydrogen peroxide.

Figure 9 shows that salinity stress (3000 ppm) and CUR-PVA nano-composite at all concentration significantly increased antioxidant enzymes activities (CAT, POX, SOD & GR) relative to control. This stimulation of CUR-PVA nano-composite was in opposite direction with its concentrations. Since, 20 mg L⁻¹ CUR-PVA

nano-composite was the most pronounced treatment. Regarding interaction between salinity stress and different concentrations of CUR-PVA nano-composite, it was noted that CUR-PVA nano-composite at all concentrations significantly increased antioxidant enzyme activities under investigation in plant watered with tap water or saline solution (3000 ppm) compared to control. Antioxidant enzymes activities (CAT, POX, SOD and GR) increased significantly at 20 mg L⁻¹ of CUR-PVA nano-composite in relative to control.

3.4 SDS-protein electrophoresis

Data in Table 5 and Fig. 10 illustrated the effect of salinity stress (3000 ppm) interacting with four different concentrations of CUR-PVA nano-composite(0, 20, 40 and 60 ppm) on protein banding patterns of sunflower plants by SDS- PAGE electrophoretic protein patterns. It was noted that 22 polypeptide bands with different molecular weights extending from 17.6.9 to 200.198 kDa were detected with polymorphic ratio 68.18%. However, all bands distributed as follow: 7 bands with molecular weights (200.198, 164.193, 107.625, 73.653, 57.197, 26.942 and 17.609 KDa) was monomorphic band (found in all samples), 9 bands with various molecular weights (188.072, 149.513, 130.849, 84.061, 63.781, 43.911, 31.919, 22.033 and 20.097 KDa) were polymorphic bands (found in more than one sample) and there were 6 unique bands (found only in one sample) with molecular

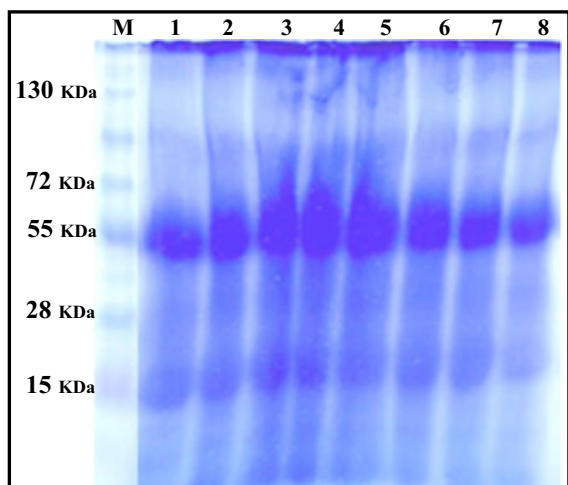


Fig. 10 Effect of CUR-PVA nano-composite concentrations (0, 20, 40 and 60 mg L⁻¹) on protein banding patterns of sunflower cultivated under salt stress (S0, water; S1, 3000 ppm). **M**= Protein Marker; **1** = control (S0, tap water); **2** = S0 + CUR-P 20; **3** = S0 + CUR-P 40; **4** = S0 + CUR-P60; **5** = Salinity (S1, 3000 mg L⁻¹); **6** = S1 + CUR-P 20; **7** = S1 + CUR-P40; **8** = S1 + CUR-P60

weights (174.001, 137.399, 126.051, 115.664, 92.422 and 40.750KDa) in treatments number (5, 8, 5, 1, 2 and 1), respectively.

4 ISSR Molecular Markers

Scored data in Table 6 and Fig. 11 showed summary results on the effect of interacting CUR-PVA nano-composite (CUR-PVA) and salinity stress on reproducible DNA fragments that identified by five ISSR primers (Table 2). Multiple fragments with different molecular weights were detected using the five ISSR primers, and the reproducible fragments distributed between monomorphic bands, polymorphic bands and unique bands.

Moreover, Table 6 shows 98 bands as total number of bands (TAF) distributed as 34 were polymorphic (PB) (95.92%) polymorphism. The maximum level of polymorphism could be detected with primers IS-04 and IS-05 which both of them exhibited 100% polymorphism, while the lowest polymorphism was at 86.67% with primer IS-01.

It was noticed that the detected bands were varied in number, polymorphism and range of its molecular weights between used ISSR primers. With regard to IS-01, 15 bands were detected with this primer and molecular weights of these bands ranged between (480.24–1221.30 bp), moreover, it distributed as 2 monomorphic bands (MB), 10 unique bands (UB) and 3 polymorphic bands (PB) with 86.67% polymorphism. Meanwhile, there were 16 bands with molecular weights (319.42–1221.30 bp) and 93.75% polymorphism were

Table 6 Effect of CUR-PVA nano-composite concentrations (0, 20, 40 and 60 mg L⁻¹) on molecular characteristics of sunflower cultivated under salt stress (S0, water; S1, 3000 ppm)

Primers	Primer Code	Marker size (bp)	Amplified bands				PB%
			TAF	MB	UB	PB	
IS-01	14 A	480.24–1221.30	15	2	10	3	86.67
IS-02	HB 8	319.42–1221.30	16	1	8	7	93.75
IS-03	HB 10	341.84–1516.92	17	1	9	7	94.12
IS-04	HB 12	466.69–1858.64	22	–	18	4	100.00
IS-05	HB 15	246.28–1855.03	28	–	15	13	100.00
Total			98	4	60	34	95.92
Average			19.6	0.8	12.0	6.8	–

TAF = Total amplified fragments, MB = Monomorphic bands, UB = Unique bands PB = Polymorphic bands and PB (%) = Percentage of polymorphism

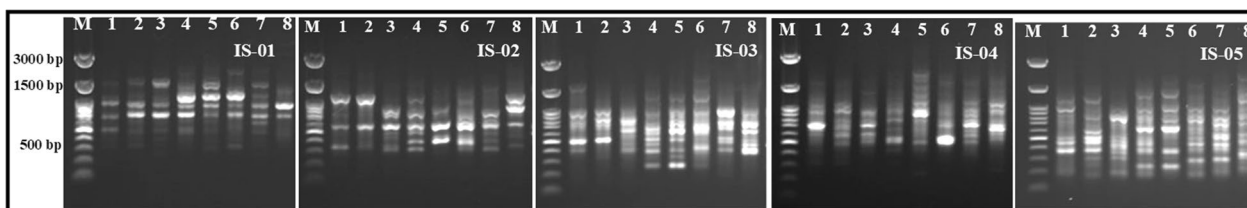


Fig 11 Effect of CUR-PVA nano-composite concentrations (0, 20, 40 & 60 mg L⁻¹) on ISSR-based PCR fragments of sunflower cultivated under salt stress (S0, water; S1, 3000 ppm). **M** = DNA Marker; **1** = control (S0, tap water); **2** = S0 + CUR-P 20; **3** = S0 + CUR-P 40; **4** = S0 + CUR-P60; **5** = Salinity (S1, 3000 mg L⁻¹); **6** = S1 + CUR-P 20; **7** = S1 + CUR-P40; **8** = S1 + CUR-P60

detected using IS-02 primer, and distributed as 1 (MB), 8 (UB) and 7 (PB). Moreover, there were 17 bands with molecular weights (341.84–1516.92 bp) and 94.12% polymorphism were detected using IS-03 primer, and distributed as 1 (MB), 9 (UB) and 7 (PB).

On the other hand, with IS-04 and IS-05, there were not any monomorphic bands, so that, the polymorphism was 100%. There were 22 and 28 bands with molecular weights (466.69–1858.64 bp) and (246.28–1855.03 bp) were detected using IS-04 and IS-05, respectively. These previous bands were distributed as (18 UB and 4 PB) and (15 UB and 13 PB) with IS-04 and IS-05, respectively.

5 Discussion

5.1 Effect of salinity

The decrease in growth indices as a result of salinity stress (Table 3) is probably attributed to osmotic stress that decreased water absorption from soil [45, 46], leading to ionic imbalance, stomatal closure, and decreased photosynthesis ratio [46]. Ashraf [47] detailed that plant growth was restricted by salinity stress via affecting various physiological and biochemical strategies (photosynthesis, nitrogen metabolism, ion homeostasis, and osmolytes accumulation) and diminishing enzymes activities of Calvin cycle [48]. Disequilibrium of water status due to salt stress caused alterations in transpiration and respiration [49]. Zhao et al. [50] and Quamruzzaman et al. [51] indicated that the disturbance of various enzymatic activities and hormonal balance affecting cell expansion, stomata closure, reducing the plant's ability to assimilate CO₂, reduced photosynthetic activity, and impairing the ability to detoxify reactive oxygen species (ROS).

The decrease in chlorophyll a and b, carotenoid and total photosynthetic pigment in plants cultivated under salt stress (Fig. 7) may be due to degradation of thylakoid membranes, chlorophyll breakdown by enhancement of the proteolytic enzymes [52]. In addition, inhibition in photosynthesis caused via accumulation of Na⁺ and Cl⁻ ions inside the chloroplast [53]. Guo et al. [54] cited that salt pressure brought about stomatal closure, brought about less CO₂ absorption, and decreased transpiration rate.

Salt stress induced increase in proline (osmoprotectant) content (Fig. 8) can be attributed to the role of proline in regulating cellular osmotic pressure, leading to enhanced water uptake and transport under salt stress [55]. Furthermore, due to its ability to scavenge free radicals, proline is elaborated in protecting cellular structures and various enzymes from oxidative damage [56]. In addition, proline plays an important role in stabilizing the three-dimensional structure of membranes and proteins and protecting subcellular structures which includes mitochondria and chloroplasts [57] and in inducing stress response genes [58].

Salinity stress significantly increased secondary metabolites as shown in Fig. 8. Phenolic compounds are antioxidants that elicit the formation of many secondary metabolites through the shikimate or malonate cycle and have cell signaling functions [59]. Furthermore, phenolic compounds may be involved in the hydrogen peroxide scavenging cascade in plant cells [9]. Flavonoids are secondary metabolites of plants that effectively scavenge oxidative molecules, including singlet oxygen and free radicals, and play important physiological roles in plant stress tolerance [10].

Regarding increments in hydrogen peroxide, malondialdehyde, antioxidant enzymes due to salinity stress as shown in Fig. 9. It is normal that salinity stress produced oxidative stress via increasing hydrogen peroxide (H₂O₂), superoxide (O⁻²) and malondialdehyde (MDA) in plant cells [60]. These increases could be attributed to insufficient induction of antioxidant systems, as suggested by Hossain et al. [61]. Oxidative damage leads to an imbalance between free radical production and cellular antioxidant defenses. Cellular damage produced by excess oxygen free radicals has been explained as a change in the cell membrane affected by the oxidation of polyunsaturated fatty acids in the lipid bilayer, a process called lipid peroxidation.

An excessive level of lipid peroxidation is probably because of failure of endogenous antioxidants to scavenge all ROS resulted from salt stress [62]. For the duration of lipids membrane peroxidation, MDA produced is typically used as a sign of oxidative damage. The excessive MDA content might result in electrolyte leakage, and loss of membrane integrity.

Chaparzadeh et al. [63] found that salinity extensively increased the activities of lipid peroxidation products (MDA) and antioxidant enzymes (superoxide dismutase; SOD, peroxidase; POX and polyphenol oxidase; PPO). In fact, the increased activity of antioxidant enzymes under salt stress may indicate the increased generation of ROS and the establishment of protective mechanisms to reduce oxidative damage caused by salt stress. Since plants usually respond to oxidative damage by increasing the activity of antioxidant enzymes, plants are shown to be stress-resistant [64]. Likewise, increased activity of SOD, POX, and CAT is connected with enhanced protection against the damaging consequences of oxidative stress [65].

Notably, SOD, CAT and peroxidase are generally recognized as main constituents of plant antioxidant defenses [66]. Represents the first line of defense against ROS [67]. Thus, the activation of antioxidant enzymes under salt conditions plays a key role in enhancing plant defenses by breaking down H₂O₂ to H₂O at different cellular locations [68]. SOD catalyzes the disproportionation of two

molecules of O^{-2} to the less toxic H_2O_2 and O_2 [69]. In addition, H_2O_2 is reduced by conversion to H_2O by POX enzymes [70]. Peroxidase enzymes are important in biochemical processes in plants to scavenge ROS and protect plant cells from H_2O_2 damage under abiotic stress [71].

5.2 Effect of CUR-PVA nano-composite

First of all, curcumin is strong anti-oxidant because of its polyphenolic nature [16, 17] and displays the free radical scavenging activity by donating H-atom from the phenolic group in acidic or neutral pH [72, 73].

Normally, phenolic compounds play tremendous position in regulation of plant metabolic processes and act as a substrate for lots antioxidant enzymes [74]. In this concern, Einhellig and Leather [75] demonstrated that phenolic compounds increased different growth parameters due to its influence on physiological processes such as cellular expansion, membrane permeability, nutrient uptake and chlorophyll synthesis. Additionally, Rice [76] and Einhellig [77] stated that phenolic acids may interfere with indole-acetic acid metabolism, mitochondrial metabolism and respiration, photosynthesis, synthesis of proteins, ion uptake and transport. Dawood and Sadak [78] revealed that the increase in phenolic compounds was coinciding with the increase in IAA contents. The total phenolic contents as diphenols and polyphenols inhibit IAA oxidase activity and leading to auxin accumulation, and reflected in stimulating the growth and yield of plant.

Moreover, two ferulic acids in CUR bound with two carboxyl groups via methylene bridges [11, 12]. Ferulic acid affects the growth of several plant species [79]. According to Milborrow [80], it has an effect on counteracting IAA decarboxylation and this could be due to its role as a modulator of transcription factors, cytokines, growth factors, enzymes, and redox status in cells. Curcumin can have various effects on transcriptional regulation; shelter DNA from damage; and prevent lipid peroxidation [81], protect DNA from damage and inhibit lipid peroxidation [82]. CUR, like many other antioxidants, scavenges a variety of reactive oxygen species (ROS) i.e. superoxide anion, the hydroxyl radical, the singlet oxygen, nitric oxide and peroxy nitrite [83–85]. Curcumin forms stable curcumin dimers when radicals bind to it and this limits ROS-induced DNA damage [86, 87]. Turmeric lowers lipid peroxidation through improving the actions of antioxidant enzymes (superoxide dismutase, catalase and glutathione peroxidase) [88]. CUR has ability to improve intracellular glutathione levels due to its antioxidant property [89].

Increasing in total chlorophylls owed to the ability of CUR to interact with DNA and mediate the transient increase in expression of enzymes of the C5 pathway for chlorophyll synthesis [90]. El-Masry and Abd El-Rahman [91] revealed that foliar application of turmeric extract at 0.05 to 0.80% significantly improved leaf area, total chlorophyll content, and leaf content of mango. Likewise, foliar spray of turmeric extract significantly increased leaf mineral content in mango trees [92], and peach [93]. Upadhyaya et al. [94] recommends that low concentration of CUR enhances arsenic induced toxicity in *Vigna radiate* through increasing germination percentage, growth parameters and photosynthetic pigments. Moreover, foliar application of Nano-curcumin (CU-NPs) expressively increased growth parameters i.e. plant height, number of branches/plant & fresh and dry weights of plants and total chlorophyll % with increasing the level of CU-NPs [95].

Regarding changes in protein banding patterns and ISSR-based PCR fragments due to effect of CUR-PVA nano-composite (CUR-PVA) and salinity stress on sunflower plants is shown in Tables 5 and 6 and illustrated in Figs. 10 and 11. Several studies showed that biochemical markers of proteins are good powerful tool for characterization of genetic diversity and differentiation among plants [96]. Moreover, combined RAPD and ISSR techniques were applied for studying genetic divergence in crops [97, 98].

Unfortunately, there is no abundant data inside the literature on the content of sunflower protein fractions. Except, one of a kind problems arose for the duration of the isolation and purification step of the main protein fraction of sunflower seeds [99]. One of the motives was the presence of extreme quantities of phenolic compounds, especially chlorogenic acid. The interaction between Phenolic compounds and proteins forms complexes which decreasing both their digestibility and functionality [100, 101]. Jasso De Rodríguez et al. [102] concluded that soluble proteins in leaves of six sunflower cultivars have different relative concentrations depending on the growing stage and sunflower variety. ISSR markers were defined as being efficient in detecting genetic diversity and genetic variation as presented by Abdalla et al. [103] and Abdul Shakoor et al. [104]. Clara et al. [105] used different ISSR primers to determine the relationship and similarity among different cultivars of sunflower and reported that Primers HB-13 and HB-15 displayed the maximum polymorphism (100%). According to Dawood et al. [106] ISSR molecular markers was used to know the molecular changes in chickpea due to interaction between proline or glycinebetaine and salinity, they found that there were a

variety of different types of polymorphic bands were detected as a response to different treatments.

6 Conclusions

It could be concluded that CUR-PVA nano-composite exerts pronounced result in decreasing the damaging effect of salinity on quality of sunflower.

6.1 Future work

1 To change the ratios of CUR in composite and investigate the stimulatory impact on plants cultivated under normal and salinity stress conditions.

2 Using electro spun method with variant core-shell using natural polymer to improve sustained release of CUR.

Acknowledgements

Not applicable

Author contributions

FSZ performed the field experiments and photosynthetic pigments analysis and chemical analysis. MAK performed the statistical analysis of recorded data and Molecular assay. MEE performed the field experiments and photosynthetic pigments analysis and chemical analysis. MGD contributed to writing, reviewing, editing and conceptualization. AEE Prepared CUR-PVA nano-emulsion. All authors Read and approved the final manuscript.

Funding

No funding was obtained for this study.

Availability of data and materials

All data generated or analyzed during this study are included in this published article.

Declarations

Ethics approval and consent to participate

Not Applicable

Consent for publication

The participants declare that the work has been consented for publication.

Competing interests

The participants declare that they have no competing interests.

Received: 2 February 2023 Accepted: 5 June 2023

Published online: 12 June 2023

References

- Rehman AU, Safer M, Qamar R, Altaf MM, Sarwar N, Farooq O, Iqbal MM, Ahmad S (2019) Exogenous application of salicylic acid ameliorates growth and yield of sunflower (*Helianthus annuus* L.) in saline soil. *Agrosciencia*. 53:207–217
- Abd El-Hameid AR, Sadak MS (2020) Impact of glutathione on enhancing sunflower growth and biochemical aspects and yield to alleviate salinity stress. *Biocatal Agric Biotechnol* 29(2020):101744
- Razzaq A, Ali A, Safdar LB, Zafar MM, Rui Y, Shakeed A, Shaikat A, Ashraf M, Gong W, Yuan Y (2020) Salt stress induces physicochemical alterations in rice grain composition and quality. *J Food Sci* 85:14–20
- Cai ZQ, Gao Q (2020) Comparative physiological and biochemical mechanisms of salt tolerance in five contrasting high land quinoa cultivars. *BMC Plant Biol* 20(70):1–15
- Yu Z, Duran X, Luo L, Dai S, Ding Z, Xia G (2020) How plant hormones mediate salt stress responses. *Trends Plant Sci* 25:1117–1130
- Kim Y-H, Khan AL, Waqas M, Lee I-G (2017) Silicon regulates antioxidant activities of crop plants under abiotic-induced oxidative stress: a review. *Front Plant Sci* 8:510
- Mansour MMF, Ali EF (2017) Evaluation of proline functions in saline conditions. *Phytochemistry* 140:52–68
- Iqbal N, Umar S, Khan NA, Khan MIR (2014) A new perspective of phytohormones in salinity tolerance: regulation of proline metabolism. *Environ Exp Bot* 100:34–42
- Ali A, Alqurainy F (2006) Activities of antioxidants in plants under environmental stress. In: Motohashi N (ed.), *The lutein-prevention and treatment for diseases*. Trans-world Research Network, India. pp187–256
- Ali Q, Ashraf M, Athar HR (2007) Exogenously applied proline at different growth stages enhances growth of two maize cultivars grown under water deficit conditions. *Pak J Bot* 39:1133–1144
- Parihar P, Singh S, Singh R, Singh VP, Prasad SM (2015) Effect of salinity stress on plants and its tolerance strategies: a review. *Environ Sci Pollut Res* 22:4056–4075
- Yazdi SR, Corredig M (2012) Heating of milk alters the binding of curcumin to casein micelles. A fluorescence spectroscopy study. *Food Chem* 132:1143–1149
- Ershadi A, Parastouei K, Khaneghah AM, Hadian Z, Lorenzo JM (2021) Encapsulation of curcumin in Persiangum nanoparticles: an assessment of physicochemical, sensory, and nutritional properties. *Coatings* 11:841
- Priyadarsini K (2014) The chemistry of curcumin: from extraction to therapeutic agent. *Molecules* 19:20091–20112
- Payton F, Sandusky P, Alworth WL (2007) NMR study of the solution structure of curcumin. *J Nat Prod* 70:143–146
- Strasser EM, Wessner B, Manhart N, Roth E (2005) The relationship between the anti-inflammatory effects of curcumin and cellular glutathione content in myelomonocytic cells. *Biochem Pharmacol* 70:552–559. <https://doi.org/10.1016/j.bcp.2005.05.030>
- Sa G, Das T, Banerjee S, Chakraborty J (2010) Curcumin: from exotic spice to modern anticancer drug. *AlAmeen J Med Sci* 3:21–37
- Anand P, Thomas SG, Kunnumakkara AB, Sundaram C, Harikumar KB, Sung B, Tharakan ST, Misra K, Priyadarsini IK, Rajasekharan KN, Aggarwal BB (2008) Biological activities of curcumin and its analogues (congeners) made by man and mother nature. *Biochem Pharmacol* 76:1590–1611
- Lopresti AL (2018) The problem of curcumin and its bioavailability: Could its gastrointestinal influence contribute to its overall health-enhancing effects? *Adv Nutr* 9(1):41–50
- Mohammed HS, Khadrawy YA, Monem AS, Amer HM, ElSherbini TM, Abd El Rahman MK (2018) Formulated curcumin nanoparticles mitigate brain oxidative stress induced by reserpine in rats. *J Bionanosc* 12(2):290–296
- Dimetry ZN, Hany MH (2016) Role of nanotechnology in agriculture with special reference to pest control. *Int J Pharm Tech Res* 9(10):121–144
- Nadakavukaren M, McCracken D (1985) *Botany: an introduction to plant biology*. West, New York
- Crucho C, Barros M (2017) Polymeric nanoparticles: a study on the preparation variables and characterization methods. *Mater Sci Eng* 80:771–784
- Ke X, Tang H, Mao HQ (2019) Effective encapsulation of curcumin in nanoparticles enabled by hydrogen bonding using flash nano-complexation. *Int J Pharm* 564:273–280
- Marin E, Briceño MI, George CC (2016) Method to produce curcumin oil-in-water nanoemulsions as templates for drug carriers. *J Biotechnol Biomater* 6:247. <https://doi.org/10.4172/2155-952X.1000247>
- Moran R, Porath D (1980) Chlorophyll determination in intact tissue using N N-dimethylformamide. *Plant Physiol* 65:478–479
- Bates LS, Waldren RP, Teare ID (1973) Rapid determination of free proline for water-stress studies. *Plant Soil* 39:205–207
- Elzaawely AA, Tawata S (2012) Antioxidant capacity and phenolic content of *Rumex dentatus* L. grown in Egypt. *J Crop Sci Biotechnol* 15(59):64

29. Chang C, Yang H, Wen CJ (2002) Estimation of total flavonoid content on propolis by two complementary colorimetric methods. *J Food Drug Anal* 10:178–182
30. Heath RL, Packer L (1968) Photoperoxidation in isolated chloroplasts: I. Kinetics and stoichiometry of fatty acid peroxidation. *Arch Biochem Biophys* 125:189–198
31. Yu CW, Murphy TM, Lin CH (2003) Hydrogen peroxide-induced chilling tolerance in mung beans mediated through ABA-independent glutathione accumulation. *Funct Plant Biol* 30:955–963
32. Chen JX, Wang XF (2006) *Plant physiology experimental guide*. Higher Education Press, Beijing, pp 24–25:55–56
33. Kumar KB, Khan PA (1982) Peroxidase and polyphenoloxidase in excised ragi (*Eleusinecoracana* cv. PR 202)leaves during senescence. *Ind J Exp Bot* 20:412–416
34. Rao MV, Paliyath G, Ormrod DP (1996) Ultraviolet B and ozone induced biochemical changes in antioxidant enzymes of *Arabidopsis thaliana*. *Plant Physiol* 110:125–136
35. Saraswati R, Matoh T, Phupaibul P, Lumpkin T et al (1993) Identification of *Sesbania* species from electrophoretic patterns of seed proteins. *Trop Agr* 70:282–285
36. Laemmli UK (1970) Cleavage of structural proteins during the assembly of the head of bacteriophage T4. *Nature* 227:680–685
37. Khaled AM K, Esh AMH (2008). High quality genomic DNA impurities-free from sugar crops and other plant tissue. In: *Proc Internl Symp on Technologies to Improve Sugar Productivity in Developing Countries*, Guilin, P.R. China: 330–332
38. Silva FAS, Azevedo CAV (2016) The assistat software version 7.7 and its use in the analysis of experimental data. *Afr J Agric Res* 11(39):3733–3740
39. Yallapua M, Jaggi M, Chauhana S (2010) Beta-cyclodextrin-curcumin self-assembly enhances curcumin delivery in prostate cancer cells. *Colloids Surf B* 79:113–125
40. Wang P, Hu W, Su W (2008) Molecularly imprinted poly (methacrylamide-co-methacrylic acid) composite membranes for recognition of curcumin. *Anal Chim Acta* 615:54–62
41. Sun X, Williams G, Hou X, Zhu L (2013) Electrospun curcumin-loaded fibers with potential biomedical applications. *Carbohydr Polym* 94:147–153
42. Liandong H, Yanhong J, Feng N, Zheng J, Xun Y, Kuiliang J (2012) Preparation and enhancement of oral bioavailability of curcumin using microemulsions vehicle. *J Agric Food Chem* 60:7137–7714
43. El-Nashar DE, Rozik NN, Soliman AM, Helaly FM (2016) Study therelease kinetics of curcumin released from PVA/curcumincomposites and its evaluation towards hepatocarcinoma. *J AppPharm Sci* 6(07):067–072
44. Rezaei A, Nasirpour A (2018) Encapsulation of curcumin using electrospun almond gum nanofibers: fabrication and characterization. *Int J Food Prop* 21(1):1608–1618
45. Mansour E, Moustafa ESA, Desoky ESM, Ali MMA, Yasin MAT, Attia A, Alsuhaibani N, Tahir MU, El-Hendawy S (2020) Multidimensional evaluation for detecting salt tolerance of bread wheat genotypes under actual saline field growing conditions. *Plants* 9:1324
46. Taha S, Seleiman R, Alhammad MF, Alkahtani BA, Alwahibi J, Mahdi MS (2021) activated yeast extract enhances growth, anatomical structure, and productivity of *Lupinustermis* L. plants under actual salinity conditions. *Agronomy* 11:74. <https://doi.org/10.3390/agronomy111010074>
47. Ashraf M (2004) Some important physiological selection criteria for salt tolerance in plants flora - morphology distribution functional. *Ecol Plants* 199(5):361–376. <https://doi.org/10.1078/0367-2530-00165>
48. Ashraf M, Shahbaz M, Ali Q (2013) Drought-induced modulation in growth and mineral nutrients in canola (*Brassica napus* L.). *Pak J Bot* 45:93–98
49. Al-Ashkar I, Alderfasi A, Ben Romdhane W, Seleiman MF, El-Said RA, Al-Doss A (2020) Morphological and genetic diversity within salt tolerance detection in eighteen wheat genotypes. *Plants* 9:287
50. Zhao C, Zhang H, Song C, Zhu J, Shabala Z (2020) Mechanisms of plant responses and adaptation to soil salinity. *Innovation* 1:100017
51. Quamruzzaman M, Manik SMN, Shabala S, Zhou M (2021) Improving performance of salt-grown crops by exogenous application of plant growth regulators. *Biomolecules* 11:788. <https://doi.org/10.3390/biom11060788>
52. Rady MM, Taha RS, Semida WM, Alharby HF (2017) Modulation of salt stress effects on *Viciafaba* L. plants grown on a reclaimed-saline soil by salicylic acid application. *Rom Agric Res* 34:175–185
53. Hasanuzzaman M, Nahar K, Rahman A, Anee TI, Alam MU et al (2017). Approaches to enhance salt stress tolerance in wheat. pp. 151–187. UK: Intech Open Limited 5 Princes Gate Court London. <https://doi.org/10.5772/67247>.
54. Guo R, Yang Z, Li F, Yan C, Zhong X et al (2015) Comparative metabolic responses and adaptive strategies of wheat (*Triticumaestivum* L.) to salt and alkali stress. *BMC Plant Biol* 15:170. <https://doi.org/10.1186/s12870-015-0546-x>
55. Oraki H, Khanjani FP, Aghaalkhna M (2012) Effect of water deficit stress on proline contents, soluble sugars, chlorophyll and grain yield of sunflower (*Helianthus annuus* L.) hybrids. *Afr J Biotechnol* 11:164–168
56. Rady MM, Sadak MS, El-Lethy SR, Abd El-Hamid EM, Abdelhamid MT (2015) Exogenous α -tocopherol has a beneficial effect on *Glycine max* (L.) plants irrigated with diluted sea water. *J Hort Sci Biotechnol* 90(2):195–202
57. Ashraf M, Foolad MR (2007) Roles of glycinebetaine and proline in improving plant abiotic stress tolerance. *Environ Exp Bot* 59:206–216
58. Chinnusamy V, Jagendorf A, Zhu JK (2005) Understanding and improving salt tolerance in plants. *Crop Sci* 45:437–448. <https://doi.org/10.2135/cropsci2005.0437>
59. Michalak A (2006) Phenolic compounds and their antioxidant activity in plants growing under heavy metal stress. *Plant Cell* 15:523–530
60. Wang Y, Li X, Li J, Bao Q, Zhang F, Tulaxi G, Wang Z (2016) Salt-induced hydrogen peroxide is involved in modulation of antioxidant enzymes in cotton. *Crop J* 4:490–498
61. Hossain MA, Mostofa MG, Fujita M (2013) Cross protection by cold-shock to salinity and drought stress-induced oxidative stress in mustard (*Brassica campestris* L.) seedlings. *Mol Plant Breed* 4:50–70
62. Rout NP, Shaw BP (2001) Salt tolerance in aquatic macrophytes: possible involvement of the antioxidative enzymes. *Plant Sci* 160:415–423
63. Chaparzadeh N, Amico MLD, Khavari-Najad RA, Izzo R, Navarizzo F (2004) Antioxidative responses of *Calendula officinalis* under salinity conditions. *Plant Physiol Biochem* 42:695–701
64. Weng M, Cui L, Liu F, Zhang M, Shan L, Yang S, Deng XP (2015) Effects of drought stress on antioxidant enzymes in seedlings of different wheat genotypes. *Pak J Bot* 47(1):49–56
65. Miller G, Suzuki N, Ciftci-yilmaz S, Mittler R (2010) Reactive oxygen species homeostasis and signalling during drought and salinity stresses. *Plant Cell Environ* 33:453–467
66. Xue FF, Liu L, Liu ZP, Mehta SK, Zhao GM (2008) Protective role of Ca against NaCl toxicity in Jerusalem artichoke by up-regulation of antioxidant enzyme. *Pedosphere* 18:766–774
67. Yahubyan G, Gozmanova M, Denev I, Toneva V, Minkov I (2009) Prompt response of superoxide dismutase and peroxidase to dehydration and rehydration of the resurrection plant *Haberleahrodopensis*. *Plant Growth Regul* 57:49–56
68. Zhu Z, Wei G, Li J, Qian Q, Yu J (2004) Silicon alleviates salt stress and increases antioxidant enzymes activity in leaves of salt-stressed cucumber (*Cucumis sativus* L.). *Plant Sci* 167:527–533
69. Gill SS, Tuteja N (2010) Reactive oxygen species and antioxidant machinery in abiotic stress tolerance in crop plants. *Plant Physiol Biochem* 48:909–930
70. Parida AK, Das AB, Mohanty P (2004) Investigations on the antioxidative defence responses to NaCl stress in a mangrove, *Bruguieraparvi* flora: differential regulations of isoforms of some antioxidative enzymes. *Plant Growth Regul* 42:213–226
71. Bowler C, Van Montagu M, Inze D (1992) Superoxide dismutase and stress tolerance. *Annu Rev Plant Physiol Plant Mol Biol* 43:83–116
72. Barclay LRC, Vinqvist MR, Mukai K, Goto H, Hashimoto Y, Tokuanga A, Uno H (2000) The antioxidant mechanism of curcumin: classical methods are needed to determine antioxidant mechanism and activity. *Org Lett* 2:2841–2843. <https://doi.org/10.1021/ol000173t>
73. Priyadarisni KI, Maity DK, Naik GH, Kumar MS, Unnikrishnan MK, Satav JG, Mohan H (2003) Role of phenolic O: H and methylene hydrogen on the free radical reaction and antioxidant activity of curcumin. *Free Radic Biol Med* 35:475–484

74. Khattab H (2007) Role of glutathione and polyadenylic acid on the oxidative defense systems of two different cultivars of canola seedlings grown under saline conditions. *Aust J Basic Appl Sci* 1(3):323–334
75. Einhellig FA, Leather GR (1988) Potentials for exploiting allelopathy to enhance crop production. *J Chem Ecol* 14(10):1829–1844
76. Rice EL (1984) Allelopathy, 2nd edn. Academic Press, Orlando
77. Einhellig FA (1986) The science of allelopathy. Wiley, pp 133–145
78. Dawood MG, Sadak MSh (2007) Physiological response of canola plants (*Brassica napus* L.) to tryptophan or benzyladenine. *Lucrari Stiintifice* 50:198–207
79. Panteli E, Voutsas E (2010) Solubilities of cinnamic acid esters in binary mixtures of ionic liquids and organic solvents. *Fluid Phase Equilib* 295(2):208–214
80. Milborrow BV (1984) Inhibitors. In: Wilkins MB (ed) *Advanced plant physiology*. Pitman Publishing, London, pp 77–110
81. Aggarwal BB, Chitra S, Nikita M, Haruyo I (2007) Curcumin: the Indian solid gold. In: Aggarwal BB, Surh YJ, Shishodia S (Eds.) *The Molecular Targets and therapeutic uses of curcumin in health and disease* pp 1–77. Library of Congress Control Number: 2006938892. ISBN-13:978-0-387-46400-8 e-ISBN-13:978-0-387-46401-5
82. Alonso J (2004) *Tratado de Fitofarmacos y Nutraceuticos*, Barcelona Corpus, p 395–403
83. Wright JS (2002) Predicting the antioxidant activity of curcumin and curcuminoids. *J Mol Struct Theo Chem* 591(1–3):207–217
84. Fujisawa S, Atsumi T, Ishihara M, Kadoma Y (2004) Cytotoxicity, ROS-generation activity and radical-scavenging activity of curcumin and related compounds. *Anticancer Res* 24:563–569
85. Menon VP, Sudheer Adhuri R (2007) Antioxidant and anti-inflammatory properties of curcumin. *Adv Exp Med Biol* 595:105–125. https://doi.org/10.1007/978-0-387-46401-5_3
86. Shalini VK, Srinivas L (1987) Lipid peroxide induced DNA damage: protection by turmeric (*Curcuma longa*). *Mol Cell Biochem* 77:3–10
87. Subramanian M, Devasagayam TP, Singh BB (1994) Diminution of singlet oxygen-induced DNA damage by curcumin and related antioxidants. *Mutat Res* 311:249–255
88. Reddy AC, Lokesh BR (1994) Studies on the inhibitory effects of curcumin and eugenol on the formation of reactive oxygen species and the oxidation of ferrous iron. *Mol Cell Biochem* 137:1–8
89. White EL, Ross LJ, Schmid SM, Kelloff GJ, Steele VE, Hill DL (1998) Screening of potential cancer preventing chemicals for induction of glutathione in rat liver cells. *Oncol Rep* 5:507–512
90. Senthil K, Sarojini R (2009) Curcumin-DNA interaction studied by fourier transform infrared spectroscopy. *Int J Biotechnol Biochem* 5:251–259
91. El-Masry SMA, Abd El-Rahman MMA (2012) Respons of taimor mango trees to foliar application of turmeric. *Minia J Agric Res Develop*. 32(5):887–899
92. Ahmed FF, Kamel MK, Ibrahim HIM (2014) The synergistic effects of using plant extracts and salicylic acid on yield and fruit quality of Keitte mango trees. *Stem Cell* 5(2):30–39
93. Al-Hadethi ME, Im AK (2015) Response of Peento peach trees to foliar spray with some plant extracts. *Zagazig J Agric Res* 42(5):1029–1034
94. Upadhyaya H, Shome S, Roy D, Bhattacharya MK (2014) Arsenic induced changes in growth and physiological responses in *Vigna radiata* seedling: effect of curcumin interaction. *Am J Plant Sci* 5:3609–3618. <https://doi.org/10.4236/ajps.2014.524377>
95. Hammam KA, Shoala T (2020) Influence of spraying Nano-curcumin and Nano-rosemarinic acid on growth, fresh herb yield, chemicals composition and postharvest criteria of French basil (*Ocimum basilicum* L. var. Grand Vert) plants. *J Agric Rural Res* 5(1):1–22
96. Jan SA, Shinwari ZK, Rabbani MA, Khurshid H, Ibrahim MI, Adil M, Ilyas M (2017) Comparison of electrophoretic protein profiles of *Brassica rapa* sub-species brown sarson through SDS-PAGE method. *Genetika* 49:95–104
97. Maloo SR, Sharma R, Devendra J, Chaudhary S, Soan H (2020) Assessment of genetic diversity in fenugreek (*Trigonella foenum-graecum*) genotypes using morphological and molecular markers. *Indian J Agric Sci* 90(1):25–30
98. Dhutmal R, Maloo SR, More A, Sharma V, Anu A, Singh VK (2021) Study of genetic diversity using molecular markers in sunflower (*Helianthus annuus*). *Indian J Agric Sci* 91(7):1058–62110
99. Durante M, Bernardi R, Lupi MC, Sabelli PA (1989) Characterization of *Helianthus annuus* L. storage proteins. *J Agric Food Chem* 37:852–855
100. Sastry MCS, Rao MSN (1090) Binding of chlorogenic acid by the isolated polyphenol-free 11S protein of sunflower (*Helianthus annuus* L.) seed. *J Agric Food Chem*. 38(12): 2103–2110
101. Žilić S, Barać M, Pešić M, Crevar M, Stanojević S, Nišavić A, Saratlić G, Tolimir M (2010) Characterization of sunflower seed and kernel proteins. *Helia* 33:103–114
102. Jasso de Rodrigue DJ, Garcia JR, Garcia RR, Sanchez JLA (2002) Characterization of proteins from sunflower leaves and seeds: Relationship of biomass and seed yield. In: Janick J, Whipkey A (eds) *Trends in new crops and new uses*. ASHS Press, Alexandria, VA
103. Abdalla MMF, Saleh HAMA, Khater MA (2020) Detection of genetic variations in *Orobancha crenata* using inter simple sequence repeat (ISSR) markers. *Bull Natl Res Centre* 44:139
104. Shakoor A, Zaib G, Zhao F, Li W, Lan X, Esfandani-Bozchaloyi S (2022) ISSR markers and morphometry determine genetic diversity and population structure in *Hedera helix* L. *Czech J Genet Plant Breed* 58(2):73–82
105. Azzam CR, Zaied KA, Abd El-Hadi AH, El-Din N, Marwa M (2019) Genetic relationships among ten sunflower inbred lines based on ISSR and RAPD analyses. *Egypt J Plant Breed* 23(4):547–563
106. Dawood MG, Khater MA, El-Awadi ME (2021) Physiological role of osmoregulators proline and glycinebetaine in increasing salinity tolerance of Chickpea. *Egypt J Chem* 64(12):7537–7548

Publisher's Note

Springer Nature remains neutral with regard to jurisdictional claims in published maps and institutional affiliations.

Submit your manuscript to a SpringerOpen® journal and benefit from:

- Convenient online submission
- Rigorous peer review
- Open access: articles freely available online
- High visibility within the field
- Retaining the copyright to your article

Submit your next manuscript at ► [springeropen.com](https://www.springeropen.com)